The 7th International Workshop on Nanotechnology and Application

IWNA 2019

6th - 9th November 2019, Phan Thiet, Vietnam

Proceedings

Organized by Vietnam National University Ho Chi Minh City
Institute for Nanotechnology
CEA - LETI - MINATEC, France

The 7th International Workshop on Nanotechnology and Application

IWNA 2019

Proceedings

6th - 9th November 2019, Phan Thiet, Vietnam

Organized by Vietnam National University Ho Chi Minh City
Institute for Nanotechnology
CEA - LETI - MINATEC, France

NMD-033-P

NUMERICAL STUDY OF AN EFFICIENT BROADBAND METAMATERIAL ABSORBER IN VISIBLE LIGHT REGION

Tran Sy Tuan,[1] Nguyen Thi Kim Thu,[1] Nguyen Thi Minh,[1] Lam Quang Hieu,[1] Nguyen Hong Quang,[1] Duong Ngoc Huyen,[2] Hugo Nguyen,[3] Nguyen Thi Quynh Hoa[1,*]

[1]Vinh University, 182 Le Duan, Vinh City, Vietnam

[2]Institute of Physics Engineering, Hanoi Univeristy of Science and Technology, Vietnam

[3]Department of Engineering Sciences, Uppsala University, Uppsala, Sweden

Email: ntqhoa@vinh.edu.vn

ABSTRACT

...e report a numerical study of a broadband metamaterial absorber in visible light region by utilizing a ...gle layer of metal-dielectric-metal configuration. The absorption bandwidth and absorption ...formances are tailored by varying the resonator shapes and metal materials. The absorption bandwidth ...f the proposed MA structure is enhanced significantly with decreasing the order of rotational symmetry ...f the resonator shape. Using gold configuration, the 2-fold symmetry MA structure based on the double-...ed axe (DSA) shaped resonator exhibits the broadband absorption response over the entire visible light ...d apart of infrared spectrum range from 320 nm to 982 nm with absorptivity above 90% for both ...nsverse electric and transverse magnetic polarizations. The physical mechanism of broadband ...sorption is explained by the current, electric and magnetic distributions, significantly affected by the ...opagating surface (PSP) and localized surface plasmon (LSP) resonances. Furthermore, the high ...sorber performances of the 2-fold symmetry MA structure can be obtained over entire visible light ...gion (400 nm - 700nm) for both noble metal of gold and low-cost metal of nickel configurations, ...dicating the proposed absorber is a promising candidate for low-cost and large-scale fabricate device ...erated in visible light region.

...ywords: Metamaterials, Visible light, Perfect absorption, Absorber.

INTRODUCTION

...Metamaterial absorber (MA) has been ...ensively studied for both theoretical research ...d practical applications since Landy et al. ...posed the microwave MA with near-unity ...sorbance in 2008 [1]. Generally, the ...tamaterial absorbers are designed based on ...e metal-insulation-metal (MIM) configuration ...cause MIM configuration can be improved the ...sorption intensity of the MA [2]. By the ...ning the shape and size of metal patch ...sonator, the MA was designed for different ...eration frequencies ranging from microwave ...optics frequencies. However, the controllable ...sign of MA to obtain a wide operation ...ndwidth, insensitivity to light polarization, ...mni-directionality, and a considerable ...duction in overall thickness has remained a ...allenging issue. Recently, many efforts have ...en recently focused on the extension of ...sorption band and control of absorption ...equency range in visible light regime for ...actical applications like photovoltaic device, photo-detector, thermal emitter, and pulse generation, etc. [3,4,5,6].

In this paper, we report a numerical study of a broadband metamaterial absorber in visible light region by utilizing a single layer of metal-dielectric-metal configuration. The absorption bandwidth and absorption performances are tailored by varying the resonator shapes and metal materials. The absorption bandwidth of the proposed MA structure is enhanced significantly with decreasing the order of rotational symmetry of the resonator shape.

EXPERIMENTAL

The proposed MA is shown in the inset of Fig. 1. MA structure consists of a periodic array of various surface geometries from asymmetry to symmetry shapes (DSA to cross, square, and circle), respectively. The top and bottom layers are made of metal materials. The different metal materials are chosen to design the MA structure including noble metals (gold and silver) and common metals (nickel and aluminum). The top

metallic layer is placed directly on the surface of a homogeneous silicon dioxide substrate. Meanwhile, the backside of dielectric layer is coved the same metallic material with the top layer acting as the ground to block the transmission. Thicknesses of the layers from top to bottom are 15 nm (t_1), 55 nm (h) and 15 nm (t_2), respectively. The geometrical dimensions of the DSA unit cell are optimized using the numerical simulation based on frequency domain solver in a Computer Simulation Technology (CST) Microwave Studio. Based on the simulated results, the optimized dimensional parameters of the unit cells for designing of the broadband MA are as follows: P = 160 nm, R = 50 nm, $R_1 = R_2$ = 30 nm, and W = 40 nm. The centers of the circles are O (x=0 nm, y=0 nm), O_1(x=35 nm, y=-35 nm), O_2(x=-35 nm, y=35 nm). The influence of structural parameters such as different structure shapes and metallic materials on the absorption characteristics of the MA is simulated and evaluated.

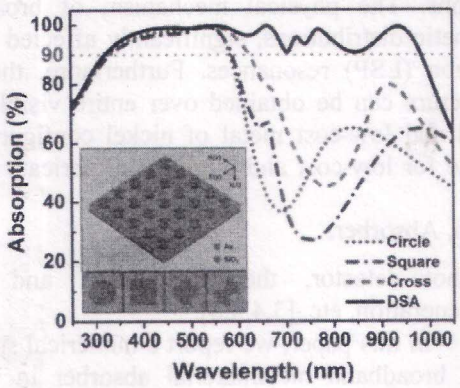

Figure 1. Absorption spectra of the proposed MA with various resonator shapes under normal incidence. The insets show the schematic of the proposed MA and top-view of various resonator shapes including circle, square, cross and double-sided axe (from left to right).

The absorption of the MA can be calculated by $A(\omega) = 1 - T(\omega) - R(\omega)$, where $A(\omega)$, $R(\omega)$ and $T(\omega)$ are the absorption, reflection, and transmission of the absorber, respectively. The transmission $T(\omega)$ and reflection $R(\omega)$ are determined from the frequency-dependent S-parameter $S_{11}(\omega)$ and $S_{21}(\omega)$, where $T(\omega) = |S_{21}(\omega)|^2$ and $R(\omega) = |S_{11}(\omega)|^2$. Because the thickness of the metal slab is thick enough to forbid the transmission of the incident wave ($T(\omega) = 0$), the absorption could be simplified to be $A(\omega) = 1 - R(\omega)$.

RESULTS AND DISCUSSION

The absorption spectra of the MAs designed with various resonator shapes under normal incidence for both transverse electric (TE) polarization are shown in Fig. 1. The absorption range of the proposed MAs can be controlled by varying the order of rotational symmetry of the resonator shapes. The largest and lowest *RAB* values are obtained in the MA with DSA and circle resonator shapes, respectively. We note that the DSA shaped MA exhibits an absorption intensity higher than 90% in a wide wavelength range of 320-960 nm, covering from UV, visible to near-infrared regions and peak absorbilities of 98.47%, 99.68%, and 99.18% in UV (~450 nm), visible (~546 nm) and near-infrared regions (~938 nm), respectively. The *RAB* of the DSA shaped MA reaches about 102%, which indicates a good wideband property.

The physical mechanism of MA is generally based on the localized surface plasmon (LSP) resonance, the propagating surface plasmon (PSP) resonance, and the combination of both the LSP and PSP resonances. The distributions of current density, electric and magnetic fields are used to explain the absorption mechanism of the MA structure. Fig. 2 shows the current density and the distributions of electric and magnetic field of the DSA-shaped MA under the TE polarization at various resonant wavelengths of 450 nm, 546 nm and 938 nm in the YOZ plane. As seen in Figs. 2(a)-(c), the current density is mainly concentrated in the metallic resonator and on top of the metallic ground plane, which confirms the surface plasmon resonance. It was reported that the surface plasmon resonance can be attributed to the wideband absorption phenomenon. Furthermore, the electric current distributes in the top and bottom metal layers that means the origins of the energy loss in the dielectric layer which results in the broadband absorption. The electric field distribution is localized around the metal corners between the neighbor unit cells, as seen in Figs. 2(d)-(f). Furthermore, the electric field is also strong coupled in to air-slot at that resonant wavelength of 938 nm, indicating that surface plasmon polaritons (SPPs) are excited in the structure. The distributions of the magnetic field at these resonant wavelengths are shown in Figs. 2(g)-(k). The distributions of the magnetic field of the MA for various resonant wavelengths are

...ficantly different. It was reported that the ...t distributions of the magnetic field is ... different types of resonances such as LSP ... PSP. At the resonant wavelength of 938 nm, ... localized magnetic field within the gap ...een the top metallic resonator and the ...allic ground plane results in LSP resonance. ...hile, the magnetic field is not only ...ulated in the metallic resonator but also ... through the neighbor unit cells at the ...ant wavelength of 450 nm, indicating that ... absorption around 450 nm results from PSP ...ance. Both the LSP and PSP resonances are ...ed at the resonant wavelength of 546 nm as ...enced by the distribution of magnetic field ... Fig. 2(h). Both the LSP and PSP resonances ... excited at the resonant wavelength of 546 ... as evidenced by the distribution of magnetic ...d in Fig. 2(h).

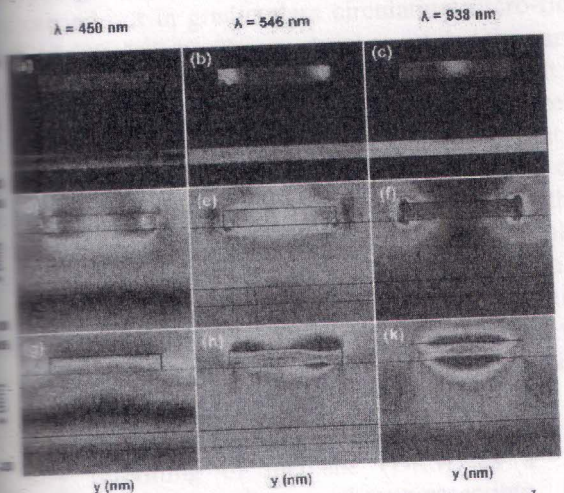

...igure 2 (a), (b), (c) Current density and ...istributions of (d), (e), (f) electric field and ...agnetic field on the YOZ plane of a unit cell at ...arious resonant wavelengths of 450 nm, 548 ...m, and 938 nm, respectively. The y-direction is ...aken form -80 nm to 80 nm.

Besides the order of rotational symmetry of ...esonator shape, the metal materials are also ...found to be affected on absorption performance ...of the MA as shown in Fig. 2. It can be observed ...that the variation of the metals not only ...influences the absorption range and bandwidth ...but also affects the absorption efficiency the ...DSA shaped MAs. Meanwhile, the absorption ...properties are almost unchanged for both TE and ...TM polarizations. The MA designed based on ...gold configuration shows the widest operating ...absorption band along with a high average ...absorption over both that band and visible light range, though these highest absorbencies are obtained for nickel configuration. We note that the DSA-shaped MAs give the average absorbance higher than 90% for both noble metals (gold and silver) and common metals (nickel and aluminum), and the nearly perfect absorbance (99%) for nickel and gold in the visible light range.

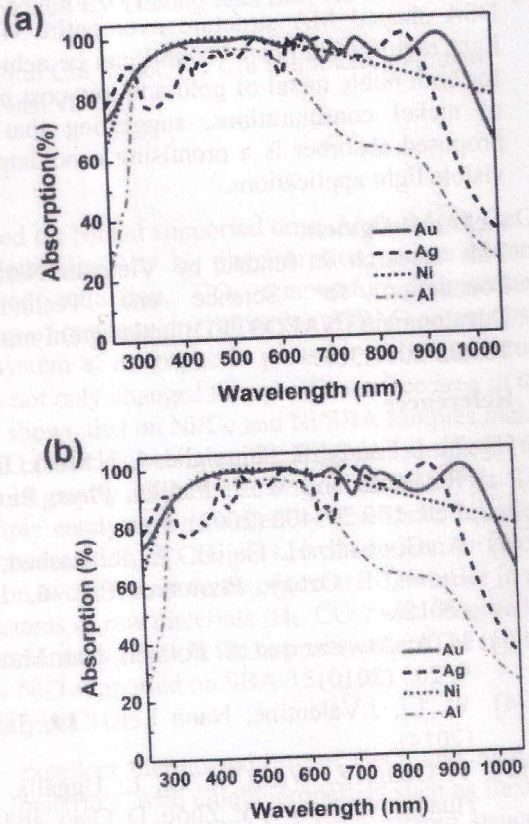

Figure 3. Absorption efficiencies of the proposed MAs designed with various metals under normal incidence for (a) TE and (b) TM polarizations.

CONCLUSION

A tailoring design of a broadband MA in visible light region based on a single layer of metal-dielectric-metal configuration was studied numerically. The absorption bandwidth and absorption performances were controlled by turning the shape and metal material of resonator shape. The absorption band was significantly increased with decreasing the order of rotational symmetry of patch resonator. Using the gold configuration, the broadband absorption response of the MA structure based on the 2-fold symmetry of the DSA shaped resonator over the entire visible light and apart of infrared

spectrum range from 320 nm to 982 nm with absorptivity above 90% for both TE and TM polarizations was obtained. The physical mechanism of broadband absorption was investigated by the current, electric and magnetic distributions, contributed by propagating surface plasmon (PSP) and localized surface plasmon (LSP) resonances. In addition, the high absorber performances of DSA shaped MA structure over entire visible light region (400 nm - 700nm) can be achieved for both noble metal of gold and low-cost metal of nickel configurations, suggesting that the proposed absorber is a promising candidate for visible light applications.

Acknowledgment

This research is funded by Vietnam National Foundation for Science and Technology Development (NAFOSTED) under grant number 103.02-2017.367.

References

[1] N. I. Landy, S. Sajuyigbe, J. J. Mock, D. R. Smith and W. J. Padilla, Phys. Rev. Lett. **100** 207402 (2008).

[2] A. Ghobadi, H. Hajian, A. R. Rashed, B Butun, E Ozbay, Photonics Res. **6**, 168 (2018).

[3] H. A. Atwater and A. Polman, Nat. Mater. **9**, 205 (2010).

[4] W. Li, J.Valentine, Nano Lett. **14**, 3510 (2014).

[5] Y. Gong, Z. Wang, K. Li, L. Uggalla, J. Huang, N. Copner, Y. Zhou, D. Qiao, and J. Zhu, Opt. Lett. **42**, 4537 (2017).

[6] T. S. Tuan and N. T. Q. Hoa, IEEE Photonics Journal **11**, 8371499 (2019).